Journal of
Civil Engineering and Structures

Journal homepage: www.journalces.com

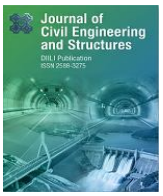

Original paper

Modeling the seismic response of gibe III dam using finite element method

Mekuanint Shitaw Yimer [1] and Elias Gebeyehu Ayele [1*]
[1]Arba Minch Water Technology Institute, Arba Minch University, Ethiopia.

ARTICLE INFO

Article history:
Received 26 August 2025
Accepted 30 November 2025

Keywords:

Gibe III dam
Finite Element Model
Seismic analysis
Nonlinear time-history analysis

ABSTRACT

In this paper, the seismic response of a gravity dam is investigated through using two-dimensional finite element model together with the nonlinear time history simulation approach. Taking Gibe III dam as a case study, numerical modeling is executed for the dam separately and along with the reservoir and the foundation using ABAQUS software. The seismic response is analyzed in terms of stresses, displacement, and cracking or tensile damages. The dam is supposed to structurally respond the maximum earthquake magnitude experienced within 150km radius of its site for the past 100 years. Concrete damaged plasticity (CDP) model is suitably applied for defining the dam concrete behavior. Acoustic elements are utilized to consider the dam-reservoir interactions. For results accuracy, validation work is carried out for the preferred modeling approach. The analysis results demonstrate the heel part of the dam experienced highest tensile stress which is nearly equal to the permissible stress of Gibe III dam. Tensile damage result confirms that the dam heel undergo tension.

DOI: https://doi.org/10.21859/jces.10163

1. Introduction

Gravity dam is known by a structure resisting the loads solely using its own weight of the material (Ali, Alam, Haque, & Alam, 2012; Naseri & Khalkhali, 2018; Parvathi, Mahesh, & Kamal, 2021; Varughese Jiji & Nikithan, 2016). And it is may be of the primary water retaining structure in the human history (S.-H. Chen, 2015). Stability of this type of dams is highly significant owing to the reason of the immense potential of life and economic losses when they collapse. While designing gravity dams, it is necessary to determine the loads required in the stability and stress analyses. The loads which may affect the design are self-weight load, water pressures, uplift pressure, temperature, silt pressures, ice pressure, earthquake forces, wind load, sub-atmospheric pressure, wave pressure and reaction of the foundation (Ali et al., 2012). Because of large amount of water is reserved by concrete gravity dam, failure of this structure may have detrimental consequences on the downstream environment (Furgani, Imperatore, & Nuti, 2012; Naseri & Khalkhali, 2018; Yamaguchi et al., 2004).

Dams which are found in seismically active sites need a critical stability analysis and it was become an issue since the early 1930s (Ali et al., 2012; S.-s. Chen, Fu, Wei, & Han, 2016; Das & Cleary, 2013). Even though this structure can resist moderate earthquakes, a difficult problem may probably happen when these structures are built in a seismically active & Dynamics, 1982) examined that significant tensile stresses which are over the strength of the concrete would be obtained in the dam body when strong earthquakes happened. Subsequently, numerous nonlinear analyses techniques have been executed for the prediction of cracks initiation and its propagations (Skrikerud, Bachmann, & dynamics, 1986; Varughese & Nikithan, 2016). Skrikerud and Bachmann (1986) carried out findings about the crack formation in the body of Koyna gravity dam during strong earthquake event. Employing the criteria of material maximum tensile strength, these researchers modelled Koyna dam's crack propagations using strong earthquake motions.

Alsuleimanagha and Liang (2012) studied the seismic behavior of Baozhusi dam against Wenchuan earthquake, the intensity of this earthquake in the dam location surpassed the design strength of the dam. They found the numerical simulation results which was compatible with the real situations happened on the dam during the earthquake event. Because of large earthquake events hit the dam site, Chen et al. (2016) investigated Zipingpu dam earthquake responses and they found that their numerical simulations were agreed with the field observations.

Gibe III dam is currently producing the largest power supply to the country; however, concern over earthquake damage to dams in Ethiopia, this dam was built in the Omo valley demands great attentions (Avery & Eng, 2012; Carr, Carr, & Crossroads, 2017;

*Corresponding author Email: elias.gebeyehu@amu.edu.et

Please cite this article as: Yimer, M.S., and Ayele, E.G. (2026). Modeling the seismic response of gibe III dam using finite element method. *Journal of Civil Engineering and Structures*, 10(1), pp. 1-8.

Yewhalaw et al., 2014). The actual seismicity of the region where dam built has shown the necessity of dam seismic response assessment. And so, employing the maximum tensile strength criteria and 2-D finite element idealization of gravity dam monolith, this paper tries to simulate the dynamic behavior of Gibe III dam using a seismic acceleration that matches well to the maximum earthquake magnitude experienced nearby the dam site.

2. Gibe III dam descriptions

Gibe III dam is a straight roller compacted concrete structure, built on a narrow valley of Omo River in Ethiopia. It is one of the largest hydropower dams in the country, located in the margin of south western part of the Main Ethiopian Rift system. The approximate geographic coordinate of Gibe III dam axis which is shown in Fig. 1 is 6°50′50″N and 37°18′5″E.

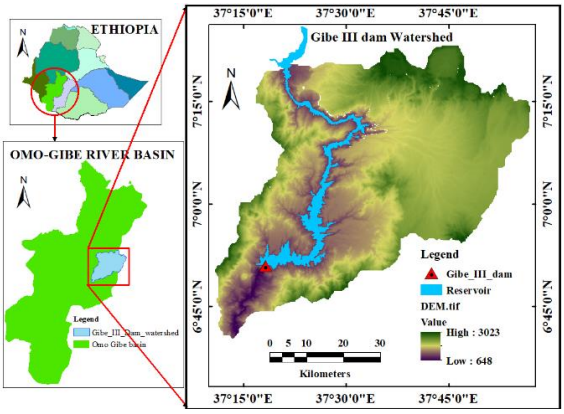

Fig 1. Gibe III dam geographical location.

Based on Gibe III dam geometry at the deepest segment of the river, the two-dimensional dam section (Fig. 2) having a 235 m height and a base width of 213 m is attached regularly to the foundation.

2.1. Seismic activity

According to Gibe III dam site seismological studies record as listed in Table 1, a maximum earthquake magnitude of 6.5 observed with in 150km radius with centering of Gibe III dam.

Table 1. Gibe III dam site seismological studies record.

Date	Epicenter	Intensity/Magnitude	Remark
1913	110km southwest	6.2Ms	ISC
1919	145km south	6.5Mw	ISC
1928	40km west	6Ms	ISC
1944	110km southeast	6Ms	ISC
1954	120km south	6.1Ms	ISC
1960	140km east	6.3Ms	ISC
1987	150km south	6.2Mw	ISC
2013	20km dam upstream	4.2Mb	ISC

ISC = International Seismological Centre

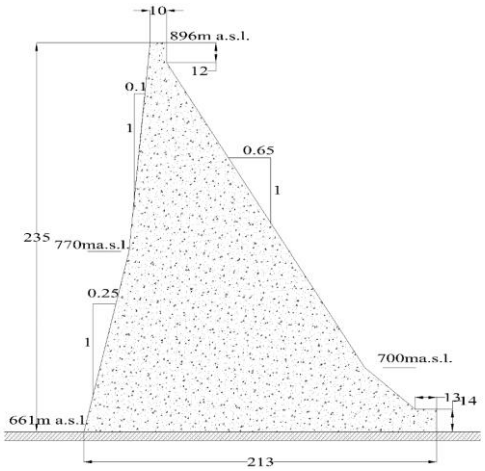

Fig 2. Geometry of non-overflow monolith of Gibe III dam, (in m).

3. Methodology and governing equations

3.1. Dynamic equilibrium equations of the dam

The system is comprised of a rigid body with mass m placed on a frictionless surface letting movement in one direction and is connected to a spring with spring constant k and a damper with damping constant c. This body is kept in motion with external applied force p letting for displacement in the direction of u, which has one natural mode of oscillation or it is a single degree of freedom system, both being time-dependent. The equation of motion, Eq. (1), governing the displacement of the idealized structure is the setup of Newton's second law of motion. Supposing inertia force $m\ddot{u}$, linear viscous damping force $c\dot{u}$ and linear elastic resisting force ku, each force is dependent on acceleration $\ddot{u}(t)$, velocity $\dot{u}(t)$ and displacement $u(t)$ respectively.

$$\mathrm{m\ddot{u}(t)} + \mathrm{c\dot{u}(t)} + \mathrm{ku(t)} = \mathrm{p(t)} \quad (1)$$

Structures subjected to seismic excitations has a total displacement,$u_t(t)$, constituted of two parts. The first one is the relative displacement between mass and ground, $u(t)$, and the next one is the ground displacement $u_g(t)$ (A. Chopra, 2012).

$$u_t(t) = u(t) + u_g(t) \quad (2)$$

The relationship is defined as Eq. (2) in a SDOF system and is then used to construct an equation of motion for seismic analysis. The second derivative is inserted and the resulting reform of Eq. (1) is observed in Eq. (3).

$$m(\ddot{u} + \ddot{u}_g) + c\dot{u} + ku = 0 \quad (3)$$

The system is without external load however the equation is often rewritten as Eq. (4) where the ground acceleration maintains motion in the system.

$$m\ddot{u} + c\dot{u} + ku = -m\ddot{u}_g \quad (4)$$

3.2. Reservoir modeling

In the present study, acoustic elements are used for the purpose of reservoir modeling. The hydrodynamic pressure developing due to the seismic acceleration of a rigid dam satisfies the wave equation, Eq. (5) which is the linear acoustic wave equation.

$$\frac{\partial^2 P}{\partial t^2} - c^2{}_w \nabla^2 P = 0 \quad (5)$$

Where, ∇^2 is the Laplace operator in two dimensions, P is the acoustic pressure and c_w is the speed of sound in water?

At the upstream far-end of the reservoir the boundary condition is set to be non-reflecting option, in which the pressure is totally absorbed (Lysmer & Kuhlemeyer, 1969). To neglect the effect of free surface wave transmission on the top layer reservoir water, the acoustic pressure is set to zero.

3.3. Structural damping

The much known Rayleigh damping is applied in the present model. Using 5% damping ratio, mass-proportional as well as stiffness-proportional damping coefficients are computed with the Eq. (6) and Eq. (7) respectively.

$$\alpha = \zeta \frac{2\omega_i \omega_j}{\omega_i + \omega_j} \quad (6)$$

$$\beta = \zeta \frac{2}{\omega_i + \omega_j} \quad (7)$$

Where, ω is the natural frequency and ζ is the critical damping ratio.

3.4. The Finite Element (FE) model

The dynamic model is implemented with an implicit-direct time integration, which is a well-known nonlinear dynamic analysis method in structural mechanics (Baig & Bathe, 2005). The 2-D finite element model of Gibe III dam is created and visualized using Abaqus/CAE, better approach for gravity dams having height (Alsuleimanagha & Liang, 2012). Two model systems are considered, the first model represents only dam system or ignoring flexible dam foundation and the second model represents the interactions of dam, reservoir and foundation. Because of the structural dimension, lane-strain elements are appropriately used to model the dam and foundation components. The Abaqus element known by CPE4R are assigned for the dam and finite region of the foundation. For the foundation far-ends (Fig. 4), the infinite Abaqus elements known by CINPE4 are implemented to propagate the waves out of the foundation and for nonreflecting of them. And for the reservoir part, the Abaqus acoustic element known

Please cite this article as: Yimer, M.S., and Ayele, E.G. (2026). Modeling the seismic response of gibe III dam using finite element method. *Journal of Civil Engineering and Structures*, 10(1), pp. 1-8.

by AC2D4 are used. For making adequate contact between the model components of dam, reservoir and foundation, appropriate mesh seed sizes and element shapes are employed (Fig. 3 and 4).

3.4.1. Material properties

Data such as dam material properties, design drawings as well as its foundation properties listed in Table 2 are obtained from the manual prepared by Gibe III dam designer Studio Pietrangeli Srl and the Ethiopian Electric Power, EEP, the owner of Gibe III hydroelectric project.

3.4.2. Concrete Damaged Plasticity (CDP) model

CDP model is one of the methods provided by the Abaqus software to represent the concrete properties and it is more than two decades since this model first obtained and improved (Lee & Fenves, 1998; Lubliner, Oliver, Oller, & Oñate, 1989). This model assumes two principal concrete failure criteria, which are tensile damage and compressive damage. The total strain tensor ε is comprised of the elastic strain tensor, ε^e and plastic strain tensor, ε^p expressed in Eq. (8).

$$\varepsilon = \varepsilon^e + \varepsilon^p \tag{8}$$

$$\varepsilon^e = E^{-1} \times \sigma \tag{9}$$

Where, E and σ correspondingly stand for the initial elastic modulus and stress tensor. ε^p Characterizes the plastic strain accounting for cracking effects. Based on plastic strain and initial stiffness of materials effective stress can be expressed as:

$$\bar{\sigma} = E_0(\varepsilon - \varepsilon^p) \tag{10}$$

$$\sigma = (1-d)\bar{\sigma} = (1-d)E_0(\varepsilon - \varepsilon^p) \tag{11}$$

Where, d varies between 0 (undamaged) and 1 (fully-damaged). The tensile behavior and damage parameter regarding the cracking strain of the concrete is provided and internally ABAQUS calculates the concrete's plastic deformation or plastic strain.

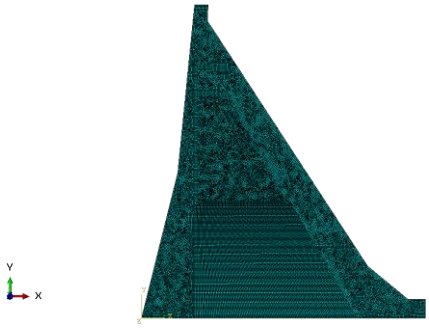

Fig 3. Mesh of the dam model.

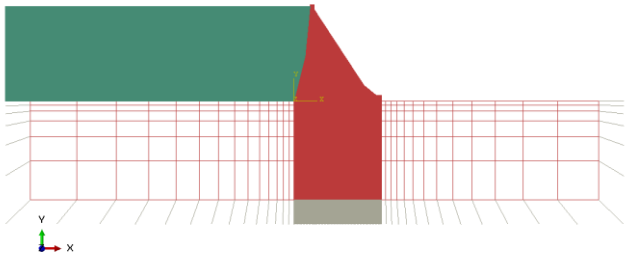

Fig 4. Mesh of the coupled FE model.

Table 2. Parameters and their values.

Part	Parameter	Value
Dam	Bulk density (ρ)	2350 kg/m³
	Poisson's ratio (ν)	0.2
	Young's modules (E)	(10 up to 20) MPa
	Tensile failure stress (t_{c0})	2.6 MPa
	Ultimate compressive stress (σ_{cu})	23 MPa
	Characteristic strength (fck)	(8 up to 18) MPa
Foundation	Bulk density (ρ)	2400 kg/m³
	Poisson's ratio (ν)	0.15
	Young's modules (E)	10 MPa
Reservoir	Density (ρ)	998.2 kg/m³
	Bulk modules (B)	2107 MPa

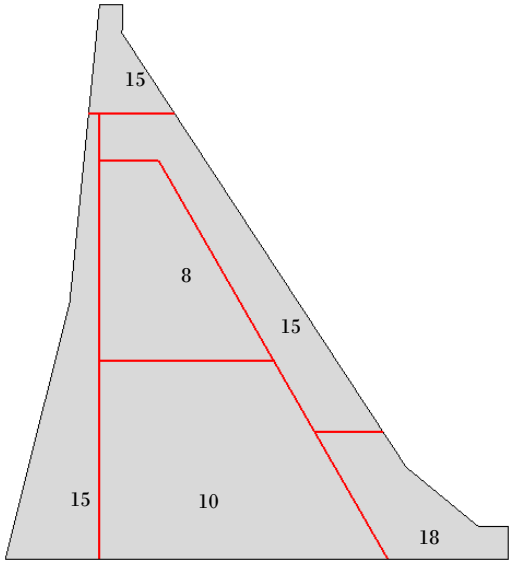

Fig 5. Dam concrete characteristic strength (f_{ck}) distribution, in MPa.

3.4.3. Loadings

Based on the site geology, foundation grouting and dam drainage activities of the Gibe III dam uplift pressure is unnoticed, as numerous scholars have done in the same manner (Akkose, Bayraktar, & Dumanoglu, 2008; Calayir & Karaton, 2005; Gao, Jin, Wang, & Wang, 2013; Khazaee & Lotfi, 2014). Thus, the applied load comprises hydrostatic pressure, hydrodynamic pressure, dam self-weight, and earthquake load. For earthquake load, the 1967 Koyna earthquake is selected based on the criteria listed in Table 3. This earthquake was recorded at the Koyna dam foundation gallery in December 11, 1967. The accelerogram of this earthquake has 10 s vibration duration and 13km distance to fault. The epicenter of this earthquake located 2 km south of Koyna dam (Chadha, Kuempel, & Shekar, 2008). Fig. 6 shows the 1967 Koyna earthquake acceleration components.

Table 3. Earthquake record selection criteria.

Criteria	Description
Tectonic environment	Medium to shallow crystal
Type of fault	Normal and strike slip
Earthquake's scenario	> 6.0 surface wave magnitude and less than 150km
Local site geology	Basalt, Trachyte, Pyroclastic or Rhyolite

Please cite this article as: Yimer, M.S., and Ayele, E.G. (2026). Modeling the seismic response of gibe III dam using finite element method. *Journal of Civil Engineering and Structures*, 10(1), pp. 1-8.

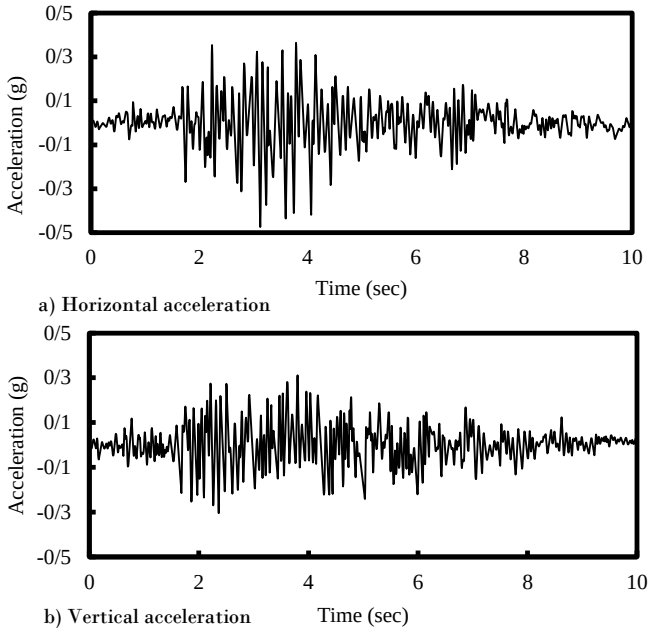

Fig 6. The 1967 Koyna earthquake, acceleration time histories.

4. Modeling validation

In numerical modeling analysis, mostly the validity of modeling system is verified by likening with the corresponding analyses which have been done before (Ghaedi, Hejazi, Ibrahim, & Khanzaei, 2018). For the current analysis, Koyna dam analyses are selected for validations as this dam has been widely studied by many researchers including (Bhattacharjee & Leger, 1993; A. K. Chopra & Chakrabarti, 1973; Ghaedi et al., 2018; Hariri-Ardebili, Seyed-Kolbadi, & Kianoush, 2016; National Research Council (US), 1990; Zhang, Wang, & Yu, 2013).

4.1. Relative dam-crest displacement

Koyna dam-reservoir-foundation modeling is carried out under the current modeling method and the relative horizontal displacement of the dam crest about its bottom is plotted, (Fig. 7).

Thus, relative horizontal crest displacement result obtained under the current modeling method is verified to the numerical study made by Zhang et al. (2013), (see Fig. 8). It is shown in Table 4 that the displacement result under current method has a satisfactory agreement with the same result of Zhang et al. (2013) analysis.

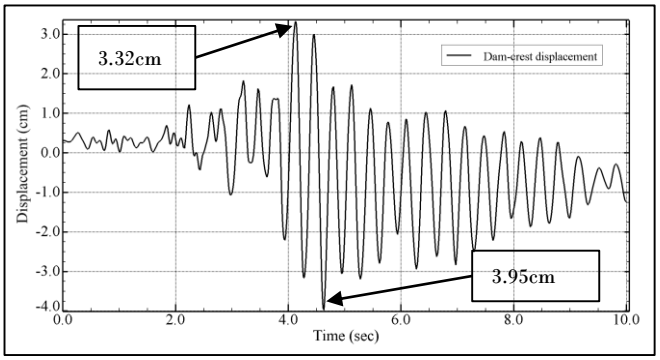

Fig 7. Koyna dam crest horizontal displacement, present method.

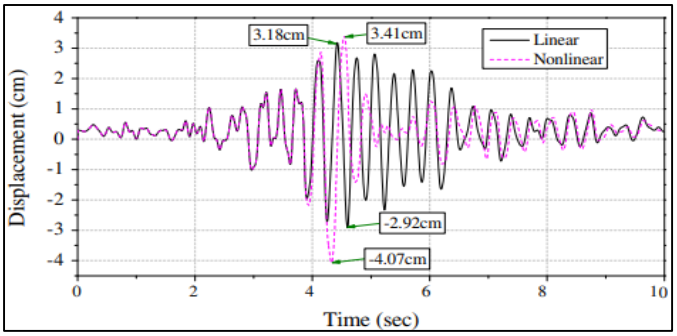

Fig 8. Koyna dam relative horizontal crest displacement, Zhang et al. (2013).

Table 4. Comparison of the relative horizontal displacement of the dam crest.

Analyses results	Crest displacement (cm) in the upstream direction	Crest displacement (cm) in the downstream direction
Current analysis result	3.95	3.32
Zhang et al. (2013) result	4.07	3.41
Difference, (in %)	3	2.7

4.2. Tensile damage and cracking

Using the present analysis method, tensile damage of Koyna dam considering dam, reservoir and foundation coupled system is investigated and the result is compared to the numerical (Ghaedi et al., 2018; Huang, 2011; Zhang & Wang, 2013; Zhang et al., 2013) and experimental (Mridha & Maity, 2014; National Research Council (US), 1990) studies illustrated in Fig. 9 and Fig. 10, respectively.

From these comparisons, the failure response of Koyna dam in the numerical studies precisely affirms to the experimental studies and to the present analysis method. Thus, the current method is well capable to predict the cracking characteristics of Koyna dam.

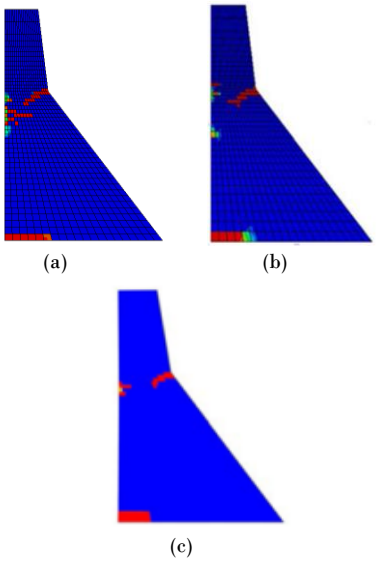

Fig 9. Numerical cracking results. (a) Present method, (b) Ghaedi et al. (2018) and (c) Huang (2011).

Please cite this article as: Yimer, M.S., and Ayele, E.G. (2026). Modeling the seismic response of gibe III dam using finite element method. *Journal of Civil Engineering and Structures*, 10(1), pp. 1-8.

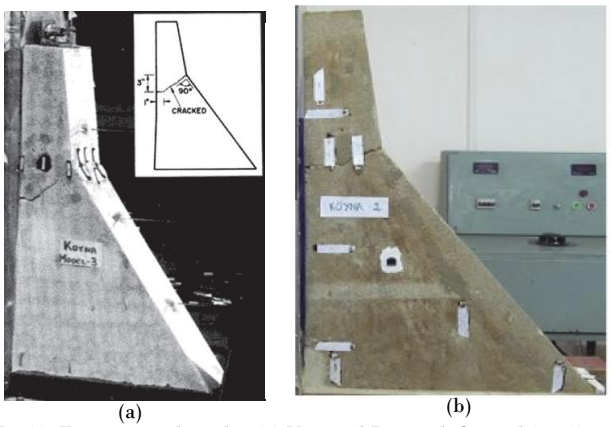

(a) (b)

Fig 10. Experimental results. (a) National Research Council (1990) and (b) Mridha and Maity (2014).

5. Results and discussions

5.1. Modal response of the dam

Modal shapes of the Gibe III dam shown in Fig. 11 are obtained using modal analysis. Table 5 illustrates the respective first four natural frequency values.

Table 5. Natural frequencies of the first 4 Gibe III dam modal shapes.

Mode	Natural frequency (Hz)
1	1.745
2	3.487
3	4.033
4	5.778

Each modal shape represents the relative displacement of all parts of the dam for that mode. While the natural frequency increases, the higher displacement is progressively shifting from the top to bottom part of the dam. At the same time, uniform displacement is seen for lower frequencies but for higher natural frequencies the body of the dam experiences no uniform displacement.

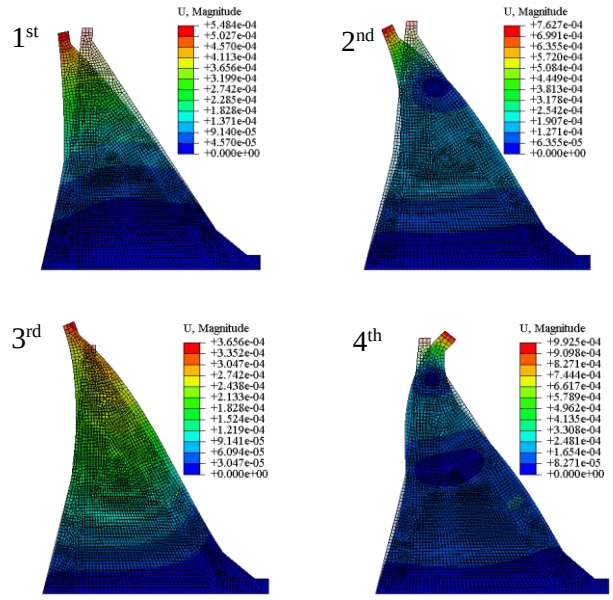

Fig 11. The first four structural resonance mode shapes of the Gibe III dam (in m).

5.2. Stress response

Because of the earthquake load intensity and dam height effect, gravity dam usually experiences higher stresses on the vertical plane or horizontal stresses (Ali et al., 2012).

5.2.1. Horizontal normal stress

In the present study, the stress contour over the vertical plane of the Gibe III dam tallest monolith is shown in Fig. 12. From this figure, the heel and crest parts of the dam suffer higher tensile stress. This confirms the inertial effect of cyclic loading on the dam due to the earthquake. The inertial force of the dam controls the higher horizontal normal stresses on the upper most parts of the dam. From the legend, maximum stress of 0.45 MPa for tension and 3.9 MPa for compression zones are obtained in the first modeling case. Similarly, maximum stress of 0.84 MPa for the tension and 4.1 MPa for compression zones are obtained in the second modeling case. From these values it can be noticed that, the joint effects of hydrodynamic pressure and flexible foundation increases the stress on the dam monolith by over 50%.

Based on USACE, (2007) guideline the obtained stress values were under the permissible stresses of Gibe III dam illustrated in Table 1.

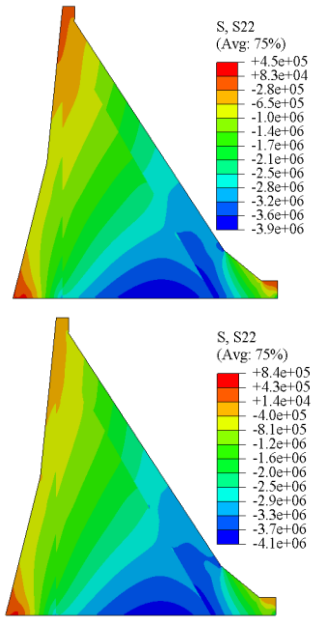

Fig 12. Horizontal normal stress contours at 10th s time step (in MPa), Left: Case-I, Right: Case-II.

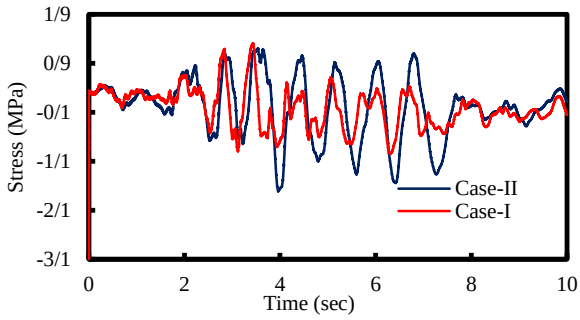

Fig 13. Normal horizontal stress versus time, node 37243 (heel part).

Horizontal normal stress response of Gibe III dam model is presented by using nodal points located at the heel (Fig. 13), upstream slope change (Fig. 14) and downstream upper slope change (Fig. 15). Maximum stress variations because of the effect of hydrodynamic pressure and deformable foundation are observed as 76%, 58% and 129% at the heel, upstream slope change and downstream upper slope change parts respectively. Thus, higher stress is developed due to the joint effect of hydrodynamic pressure and deformable foundation.

5.2.2. Dam-bottom stress distribution

Dam foundation interface is one of the critical failure locations during earthquake loading conditions. Maximum principal stress distribution along the dam bottom nodes, starting from the heel up to the toe is presented in Fig. 16. Starting from the heel up to 38 m towards the downstream, the dam bottom nodes experiences tensile stress. Stress variations in both tension and compression zones are observed because

of hydrodynamic pressure and deformable foundation, with a maximum variation of 22.7%.

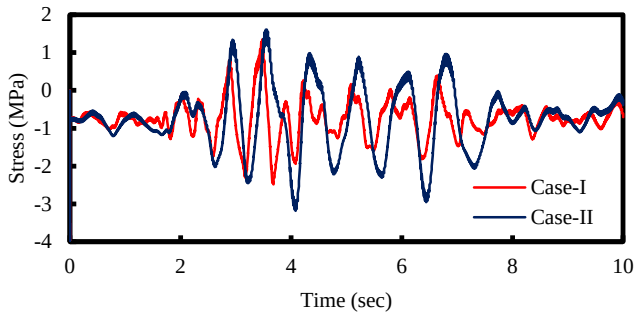

Fig 14. Normal horizontal stress versus time, node 32341 (u/s slope change).

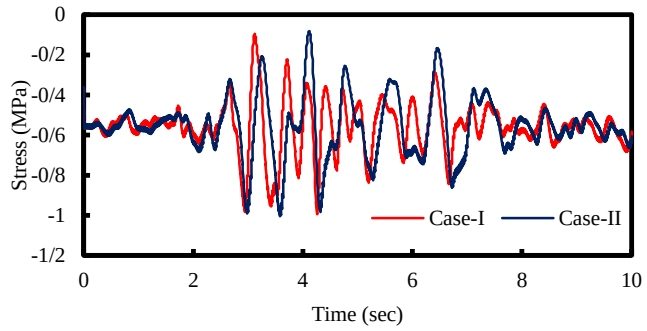

Fig 15. Normal horizontal stress versus time, node 22043 (d/s upper **slope change).**

5.3. Displacement response

The displacement contour plots of the Gibe III dam model are presented in Fig. 17. Horizontal displacement varies uniformly from bottom to top of the dam, but no uniformly for vertical displacement.

Time history of crest-heel relative horizontal displacement (Fig. 18) and vertical displacement (Fig. 19) are obtained from the analysis. Maximum horizontal displacement of the dam-crest relative to the dam-heel is obtained 7.4 cm in the case-I modeling and 9.3 cm in the case-II modeling to the downstream direction. Similarly, maximum vertical displacement of dam-crest relative to the dam-heel is obtained 2.0 cm in the case-I modeling and 2.2 cm in the case-II modeling to the downward direction.

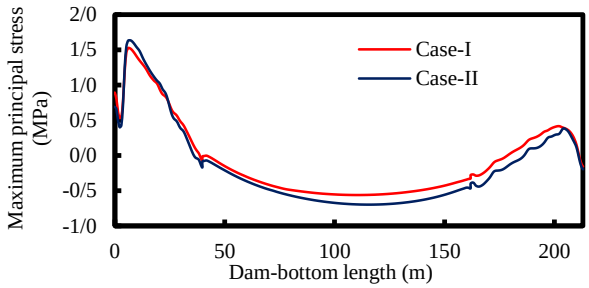

Fig 16. Maximum principal stress at the dam-bottom interface, at the 10th s time step.

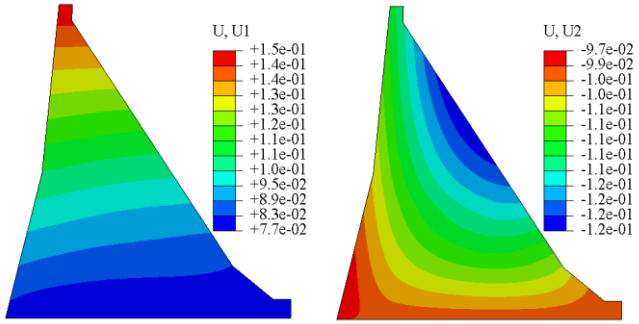

Fig 17. Displacement contours, Left: horizontal, Right: vertical, 10th s time step.

5.4. Tensile damage and cracking response

In many literatures, it has been discussed that several part of concrete dam may suffer tensile damage with subsequent crack formation during earthquake loadings. Cracking is assumed to occur when the concrete tensile strength is less than the tensile stress developed. Contour plots of tensile damage responses of Gibe III dam are shown in Fig. 20. In both modeling cases, tensile damage happened at the dam-heel area and the damage extent of case-II modeling is a little higher. According to the stress responses discussed above, near the heel part the dam experiences higher magnitude of tensile stress and reduces as it goes downstream up to 38m. Thus, the cracking and its length depends on this tensile damage result.

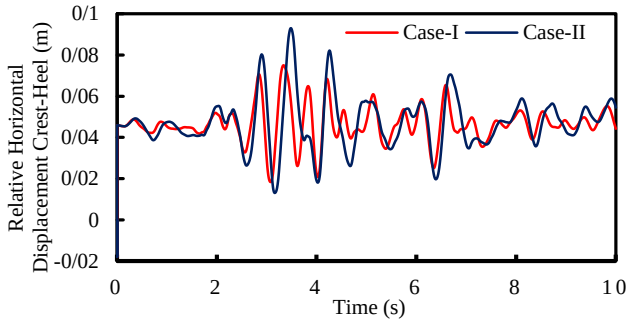

Fig 18. Time history graph of relative horizontal displacement crest-heel.

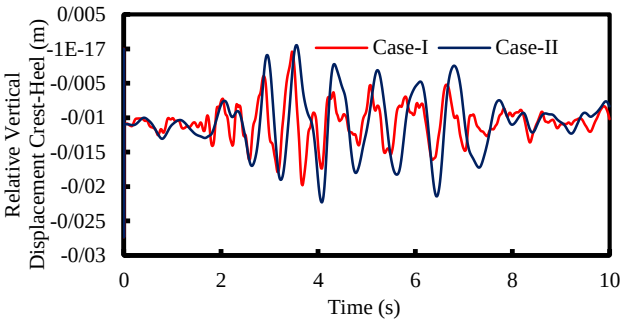

Fig 19. Time history graph of relative vertical displacement crest-heel.

Please cite this article as: Yimer, M.S., and Ayele, E.G. (2026). Modeling the seismic response of gibe III dam using finite element method. *Journal of Civil Engineering and Structures*, 10(1), pp. 1-8.

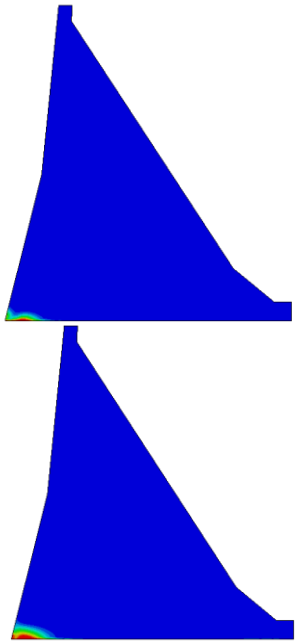

Fig 20. Dam tensile damage (cracking) evolution, Left: Case-I, Right: Case-II, 10^{th} s time step.

6. Findings

In this modeling study, determination of dynamic behavior of Gibe III dam has been made with the nonlinear finite element modeling technique. Aiming to assess the joint effects of hydrodynamic pressure and flexible foundation on the seismic or dynamic behavior of the dam, two modeling cases were applied, case-I without considering flexible foundation and hydrodynamic pressure; case-II considering flexible foundation and hydrodynamic pressure. Reservoir modeling is executed with Abaqus acoustic elements, whereas RCC dam and foundation modeling are executed with plain strain elements. The dam material nonlinear behavior is assigned with concrete damaged plasticity (CDP) model. For work accuracy, the results obtained from the nonlinear dynamic implicit modeling are compared with the reported literature and reasonably matched. In general, the major findings of the present modeling study are summarized in these manners:

1) The stress responses of the analysis are presented with contour plots or envelops and graphs. The stress spatial distribution on the dam showed that the crest and heel parts are under tension. At the heel, the highest tensile stress magnitude is read which is nearly equal to the dam permissible stress.
2) The Gibe III dam-crest displaces for about 7.4 cm in the case-I modeling and 9.3 cm in the case-II modeling horizontally to the downstream direction. It displaces for about 2.0 cm in the case-I modeling and 2.2 cm in the case-II modeling vertically to the downward direction.
3) The crack prone region is identified and it is only at the dam-heel section. The critical crack length is obtained for the initiated crack location and it extends up to 30 m. It is found that no crack initiations appeared on the other parts of the dam.
4) In general, it is observed in all result discussions that the combined effect of hydrodynamic pressure and flexible foundation has direct impact on the dynamic dam behavior.

Acknowledgement
The authors acknowledge the financial support provided by the Arba Minch Water Technology Institute.

Conflict of interest
There is not conflict of interest.

References

[1] Akkose, M., Bayraktar, A., & Dumanoglu, A. A. (2008). Reservoir water level effects on nonlinear dynamic response of arch dams. *Journal of Fluids and Structures, 24*(3), 418-435. doi:https://doi.org/10.1016/j.jfluidstructs.2007.08.007
[2] Ali, M. H., Alam, M. R., Haque, M. N., & Alam, M. J. (2012). Comparison of design and analysis of concrete gravity dam.
[3] Alsuleimanagha, Z., & Liang, J. (2012). Dynamic analysis of the Baozhusi dam using FEM. In.
[4] Avery, S., & Eng, C. J. A. S. C., the University of Oxford. (2012). Lake Turkana & the Lower Omo: hydrological impacts of major dam and irrigation developments.
[5] Baig, M. M. I., & Bathe, K.-J. (2005). *On direct time integration in large deformation dynamic analysis.* Paper presented at the 3rd MIT conference on computational fluid and solid mechanics.
[6] Bhattacharjee, S., & Leger, P. (1993). Seismic cracking and energy dissipation in concrete gravity dams. *Earthquake Engineering & Structural Dynamics, 22*(11), 991-1007.
[7] Calayir, Y., & Karaton, M. (2005). A continuum damage concrete model for earthquake analysis of concrete gravity dam–reservoir systems. *Soil Dynamics and Earthquake Engineering, 25*(11), 857-869. doi:https://doi.org/10.1016/j.soildyn.2005.05.003
[8] Carr, C. J., Carr, C. J. J. R. B. D., & Crossroads, H. R. i. E. A. A. P. (2017). The Seismic Threat to the Gibe III Dam: A Disaster in Waiting. 43-52.
[9] Chadha, R. K., Kuempel, H.-J., & Shekar, M. (2008). Reservoir Triggered Seismicity (RTS) and well water level response in the Koyna–Warna region, India. *Tectonophysics, 456*(1-2), 94-102.
[10] Chen, S.-H. (2015). *Hydraulic structures*: Springer.
[11] Chen, S.-s., Fu, Z.-z., Wei, K.-m., & Han, H.-q. (2016). Seismic responses of high concrete face rockfill dams: A case study. *Water Science and Engineering, 9*(3), 195-204. doi:https://doi.org/10.1016/j.wse.2016.09.002
[12] Chopra, A. (2012). Dynamics of Structures, Theory and Applications to Earthquake Engineering. In: Upper Saddle River: Pearson-Prentice Hall.
[13] Chopra, A. K., & Chakrabarti, P. (1973). The Koyna earthquake and the damage to Koyna dam. *Bulletin of the Seismological Society of America, 63*(2), 381-397.
[14] Chopra, A. K., Gupta, S. J. E. E., & Dynamics, S. (1982). Hydrodynamic and foundation interaction effects in frequency response functions for concrete gravity dams. *10*(1), 89-106.
[15] Das, R., & Cleary, P. (2013). A mesh-free approach for fracture modelling of gravity dams under earthquake. *International Journal of Fracture, 179*, 9-33.
[16] Furgani, L., Imperatore, S., & Nuti, C. (2012). *Seismic assessment methods for concrete gravity dams.* Paper presented at the Proceedings of the 15 WCEE, 15th World Conference on Earthquake Engineering, Lisbon, Portugal.
[17] Gao, Y., Jin, F., Wang, X., & Wang, J. (2013). Finite Element Analysis of Dam–Reservoir Interaction Using High-Order Doubly Asymptotic Open Boundary. In *Seismic Safety Evaluation of Concrete Dams* (pp. 173-198): Elsevier.
[18] Ghaedi, K., Hejazi, F., Ibrahim, Z., & Khanzaei, P. (2018). Flexible Foundation Effect on Seismic Analysis of Roller Compacted Concrete (RCC) Dams Using Finite Element Method. *KSCE Journal of Civil Engineering, 22*(4), 1275-1287. doi:10.1007/s12205-017-1088-6
[19] Hariri-Ardebili, M., Seyed-Kolbadi, S., & Kianoush, M. (2016). FEM-based parametric analysis of a typical gravity dam considering input excitation mechanism. *Soil Dynamics and Earthquake Engineering*, 22-43.
[20] Huang, J. (2011). Seismic Response Evaluation of Concrete Gravity Dams Subjected to Spatially Varying Earthquake Ground Motions. (Doctorial degree), Drexel University
[21] Khazaee, A., & Lotfi, V. (2014). Application of perfectly matched layers in the transient analysis of dam–reservoir systems. *60*, 51-68.
[22] Lee, J., & Fenves, G. L. (1998). Plastic-damage model for cyclic loading of concrete structures. *Journal of engineering mechanics, 124*(8), 892-900.
[23] Lubliner, J., Oliver, J., Oller, S., & Oñate, E. (1989). A plastic-damage model for concrete. *International Journal of solids and structures, 25*(3), 299-326.
[24] Lysmer, J., & Kuhlemeyer, R. L. J. J. o. E. M.-a. (1969). Finite Dynamic Model for Infinite Media. *95*, 859-877.
[25] Mridha, S., & Maity, D. (2014). Experimental investigation on nonlinear dynamic response of concrete gravity dam-reservoir system.

Please cite this article as: Yimer, M.S., and Ayele, E.G. (2026). Modeling the seismic response of gibe III dam using finite element method. *Journal of Civil Engineering and Structures*, 10(1), pp. 1-8.

Engineering Structures, *80*, 289-297. doi:https://doi.org/10.1016/j.engstruct.2014.09.017

[26] Naseri, F., & Khalkhali, A. B. (2018). Evaluation of Seismic Performance of Concrete Gravity Dams Under Soil-structure-reservoir Interaction Exposed to Vertical Component of Near-field Earthquakes During Impounding (Case study: Pine Flat Dam). *Journal of Civil Engineering and Materials Application*, *4*, 181-191. doi:doi: 10.22034/JCEMA.2018.91999

[27] National Research Council (US). (1990). *Earthquake engineering for concrete dams: design, performance, and research needs*. Washington (DC): National Academies Press;

[28] Parvathi, I. S., Mahesh, M., & Kamal, D. R. J. M. T. P. (2021). Critical crack lengths of concrete gravity dam by using fracture mechanics. *38*, 3149-3159.

[29] Skrikerud, P. E., Bachmann, H. J. E. e., & dynamics, s. (1986). Discrete crack modelling for dynamically loaded, unreinforced concrete structures. *14*(2), 297-315.

[30] Varughese, J. A., & Nikithan, S. J. A. i. C. D. (2016). Seismic behavior of concrete gravity dams. *1*(2), 195-206.

[31] Varughese Jiji, A., & Nikithan, S. (2016). Seismic behavior of concrete gravity dams. *Advances in Computational Design*, *1*(2), 195-206. doi:10.12989/ACD.2016.1.2.195

[32] Yamaguchi, Y., Hall, R., Sasaki, T., Matheu, E., Kanenawa, K.-i., Chudgar, A., & Yule, D. (2004). *Seismic performance evaluation of concrete gravity dams.* Paper presented at the Proceedings of the 13th World Conference on Earthquake Engineering.

[33] Yewhalaw, D., Hamels, S., Getachew, Y., Torgerson, P., Anagnostou, M., Legesse, W., . . . Speybroeck, N. J. E. R. (2014). Water resource developments in Ethiopia: potential benefits and negative impacts on the environment, vector-borne diseases, and food security. *22*(4), 364-371.

[34] Zhang, S., & Wang, G. (2013). Effects of near-fault and far-fault ground motions on nonlinear dynamic response and seismic damage of concrete gravity dams. *Soil Dynamics and Earthquake Engineering*, *53*, 217-229.

[35] Zhang, S., Wang, G., & Yu, X. (2013). Seismic cracking analysis of concrete gravity dams with initial cracks using the extended finite element method. *Engineering Structures*, *56*, 528–543. doi:http://dx.doi.org/10.1016/j.engstruct.2013.05.037

Please cite this article as: Yimer, M.S., and Ayele, E.G. (2026). Modeling the seismic response of gibe III dam using finite element method. *Journal of Civil Engineering and Structures*, 10(1), pp. 1-8.